SIViP
DOI 10.1007/s11760-017-1058-y

ORIGINAL PAPER

Compensatory fuzzy mathematical morphology

Agustina Bouchet[1] · Juan I. Pastore[1] · Marcel Brun[1] · Virginia L. Ballarin[1]

Received: 6 July 2016 / Revised: 12 September 2016 / Accepted: 4 January 2017

Abstract In this paper, we propose the use of compensatory fuzzy logic to extend mathematical morphology (MM) operators to gray-level images, in a similar way than fuzzy logic is used, naming it compensatory fuzzy mathematical morphology (CFMM). We study the compliance with the four principles of quantification and analyze the robustness of these operators by comparing them with Classic MM and fuzzy mathematical morphology (FMM), in the context of the processing of magnetic resonance images under noisy conditions. We observed that operators of CFMM are more robust, relative to noise, than MM and FMM ones, for the type of images used. As an additional result of this work, we developed a library for CFMM operators, plus an additional graphical user interface, which brings together the new operators with a wide range of operators of FMM and Classic MM.

Keywords Mathematical morphology · Fuzzy mathematical morphology · Compensatory fuzzy logic · Segmentation · Medical images

✉ Agustina Bouchet
abouchet@fi.mdp.edu.ar

Juan I. Pastore
jpastore@fi.mdp.edu.ar

Marcel Brun
mbrun@fi.mdp.edu.ar

Virginia L. Ballarin
vballari@fi.mdp.edu.ar

1 ICYTE, CONICET - UNMDP, Universidad Nacional de Mar del Plata, Mar del Plata, Argentina

1 Introduction

Mathematical morphology (MM) is a theory proposed originally for the characterization of structural properties of some materials, based on photographic images [25,26]. Geometric structures in these images are analyzed using nonlinear operations, allowing the measurement of their shape, size and orientation. A key aspect of MM is the *probing* of the images by small sets, named structuring elements (SE). On the other hand, the theory of Fuzzy Sets found promising applications in Digital Image Processing, existing, actually, a variety of tools and methods where it was applied with satisfactory results [3]. One of these applications is in the Fuzzy Mathematical Morphology (FMM), which extends basic binary operators, like erosions and dilations, to gray-level images [2]. Additionally, *pseudo-morphologies* are mathematical morphology frameworks that lack some of the theoretical properties of MM, like adjunctions, in order to improve on some other properties, like efficiency or robustness. As example of well-known pseudo-morphologies are those defined for color images which compute the extrema of the pixels at the window, without using a total ordering of the color vector values. Despite not respecting all the theoretical properties of MM, they can be of interest in various situations [1,12]. In this direction, a definition of gray-level morphological operators based on Compensatory Fuzzy Logic, named Compensatory Fuzzy Mathematical Morphology (CFMM), was presented in a preliminary work [5]. It provided improvements over other extensions of MM based on Fuzzy Sets [5]. In this work, we describe a complete formalization of such extension, showing its compliance with the four principles of quantification in R^n defined by Serra [25], and study its robustness, against noise, relative to classic MM and previously defined FMM operators. Regarding the last part, the performance of the operators was assessed on magnetic reso-

Published online: 18 January 2017

nance images (MRI), since the medical imaging field is ideal for the application of fuzzy techniques, and in particular, the generation mechanisms of MRI images result in imprecision in the definition of the borders between different structures or tissues [3], which is a situation where fuzzy operators show to be more robust [5]. In addition, a library of CFMM operators, and a graphical user interface, were developed, bringing together a wide range of operators of FMM and MM. The software allows for full parameterizations and provides display of the results, to support prototyping and learning. It also includes general techniques of image processing, such as enhancement techniques and logical and algebraic operations, as a complement to the morphological operators.

2 Fuzzy mathematical morphology

The Fuzzy mathematical morphology (FMM) is an extension of the binary MM to gray-level images, by replacing set operations by fuzzy set operations [2,13,14]. FMM is based on Fuzzy Logic and is already able to solve several problems in image processing. The main idea behind the FMM lies on the extension of inclusion and intersection, from the Boolean domain $\{0, 1\} \times \{0, 1\}$ to $\{0, 1\}$, used in binary morphology, to implications and conjunctions, which are functions from the rectangle $[0, 1] \times [0, 1]$ to $[0, 1]$. In this approach, gray-level images are represented as fuzzy sets, but it does not mean that they need to be interpreted actually as being fuzzy. The operations between fuzzy sets are defined from the operations of conjunction and disjunction on the membership values for such sets [16].

In this work, μ and ν indicate two fuzzy sets, with membership functions $\mu : U_\mu \subset R^2 \rightarrow [0, 1]$ and $\nu : U_\nu \subset R^2 \rightarrow [0, 1]$, respectively, where the first one corresponds to the gray-level image under study and the second one to the fuzzy SE. There are several approaches, developed by different authors in the literature, which study the extension of binary basic MM operators to gray-level images using fuzzy set theory [2,13–15,19,22]. Bloch and Maître achieved the unification of all these approaches, based on t-norms and s-norms [2]. We describe here the basic FMM operators as defined there. The *fuzzy dilation* of the image μ by the SE ν is defined as:

$$\delta(\mu, \nu)(x) = \sup_{y \in U_\nu} [t(\mu(y), \nu(y - x))] \tag{1}$$

where $t(a, b)$ is a t-norm [20,21].

The *fuzzy erosion* of the image μ by the SE ν is defined as:

$$\varepsilon(\mu, \nu)(x) = \inf_{y \in U_\nu} [I(\mu(y), \nu(y - x))] \tag{2}$$

where $I(a, b)$ is a fuzzy implication [22].

Since $I(a, b) = s(N(a), b)$, Eq. 2 can be rewritten equivalently as follows:

$$\varepsilon(\mu, \nu)(x) = \inf_{y \in U_\nu} [s(\mu(y), N(\nu(y - x)))] \tag{3}$$

where $s(a, b)$ is a s-norm, dual to t, and $N(a)$ is the fuzzy complement [20].

3 Advances in compensatory fuzzy mathematical morphology

This section presents a description of the advances on the topic of the CFMM. In the first part, we will describe the CFMM based on the geometric mean. Next, we will define the new Compensatory Logic based on arithmetic mean, and its use in the definition of a new CFMM based on the arithmetic mean. Then, we describe the implementation of a Matlab library, and a GUI-based program for image processing, completely developed in Matlab©. In the final part of this section, we show some application of the new operators to problems of biomedical images segmentation.

3.1 CFMM based on the geometric mean

Fuzzy logic may be viewed as an attempt to formalize the human ability to make rational decisions in environments of imprecision, uncertainty, incompleteness of information, conflicting information, and partiality of truth [27]. Two main features of fuzzy logic are a) the associative property of the conjunction and disjunction operators, and b) the absence of compensation of the truth values of the basic predicates, when computing true values for complex predicates. However, when modeling a problem where predicates do not have the same relevance, it is desirable to compensate truth values of the basic predicates, and for that it is also necessary to lose the associative property. These needs are solved by the use of non-associative multivalent logic systems, which allow for truth value compensation between basic predicates [17]. Compensatory Fuzzy Logic (CFL) is a multi-valued logic model that removes classic axioms to attain a system which is sensitive and idempotent, and compensates the predicates. Basically, for fuzzy logic, the truth value of a conjunction is always smaller or equal than the truth values of its components, and the truth value of a disjunction is always greater or equal than them. The removal of these two constraints is the foundation of the CFL. The decrease of the truth value in a component variable is compensated by the increase in another variable, allowing for higher values on the conjunction. The same behavior can be seen in disjunctions. This behavior makes the logic more sensitive to its variables [17,18]. Formally, a CFL is a quadruple

(C, D, O, N) of continuous operators, a conjunction $C : [0, 1]^n \to [0, 1]$, a disjunction $D : [0, 1]^n \to [0, 1]$, an order $O : [0, 1]^2 \to [0, 1]$ and a negation $N : [0, 1] \to [0, 1]$, that satisfy a set of axioms listed below. Let $x = (x_1, x_2, ..., x_n)$, $y = (y_1, y_2, ..., y_n)$ and $z = (z_1, z_2, ..., z_n)$ be elements in $[0, 1]^n$, the operators must satisfy the following properties [18]:

(a) Compensation: $\min\{x_1, x_2, \ldots, x_n\} \leq C(x) \leq \max\{x_1, x_2, \ldots, x_n\}$
(b) Commutative: $C(x_1, \ldots, x_i, \ldots, x_j, \ldots, x_n) = C(x_1, \ldots, x_j, \ldots, x_i, \ldots, x_n)$
(c) Strictly Increasing: If $x_1 = y_1, x_2 = y_2, ..., x_{i-1} = y_{i-1}, x_{i+1} = y_{i+1}, ..., x_n = y_n$ are nonzero, and $x_i > y_i$ then $C(x) > C(y)$
(d) Veto: If $x_i = 0$ for some i, $1 \leq i \leq n$ then $C(x) = 0$
(e) Fuzzy Reciprocity: $O(x, y) = N[O(y, x)]$
(f) Fuzzy Transitivity: If $O(x, y) \geq 0.5$ and $O(y, z) \geq 0.5$ then $O(x, z) \geq \max\{O(x, y), O(y, z)\}$
(g) De Morgan Laws: $N[C(x_1, x_2, \ldots, x_n)] = D(N(x_1), N(x_2), \ldots, N(x_n)) N[D(x_1, x_2, \ldots, x_n)] = C(N(x_1), N(x_2), \ldots, N(x_n))$

The compensatory axiom differentiates the CFL from the more general Fuzzy Logic [18]. The original definition of CFL, named Geometric Mean Based Compensatory Fuzzy Logic (GMBCFL), is based on the geometrical mean, and its dual, to define conjunction and disjunction operators [17]. Equations 4–7 define the four operators of this compensatory fuzzy logic:

$$C(x) = (x_1 \times x_2 \times \cdots \times x_n)^{\frac{1}{n}} \tag{4}$$

$$D(x) = 1 - [(1 - x_1) \times (1 - x_2) \times \cdots \times (1 - x_n))]^{\frac{1}{n}} \tag{5}$$

$$O(x, y) = 0,5[C(x) - C(y)] + 0,5 \tag{6}$$

$$N(x_i) = 1 - x_i \tag{7}$$

Based on the CFL, we presented in [5] a pseudo MM, called compensatory fuzzy mathematical morphology, where the t-norms and s-norms of the FMM, used in Eqs. 1 and 2, were replaced by the compensatory operators of conjunction and disjunction. This way, the compensatory dilation and erosion of the image μ by the SE ν are defined, respectively, as:

$$\delta(\mu, \nu)(x) = \sup_{y \in U_\nu} [C(\mu(y), \nu(y - x))] \tag{8}$$

$$\varepsilon(\mu, \nu)(x) = \inf_{y \in U_\nu} [I(\nu(y - x), \mu(y))] \tag{9}$$

where C is the compensatory conjunction and I is the compensatory implication defined as $I(a, b) = D(N(a), b)$ with N the negation operator of Eq. 7. It is important to note that the order operator O is not used in the definition of the morphological operators, but it is necessary for a complete definition of the CFL.

3.2 CFMM based on the arithmetic mean

Previous work on Compensatory Logic was based on a set of rules, defining which properties a Fuzzy Logic needed to comply with, to be compensatory, and a explicit definition of the Geometric Mean Based Compensatory Logic [17,18], which did indeed comply with the requirements. In [6], we proved that there are indeed more Fuzzy Logics complying with these requirements, defining the Arithmetic Mean Based Compensatory Fuzzy Logic (AMBCFL), based on a quartet of operators (C, D, O, N), where C and D are replaced by:

$$C(x) = \left[\min(x_1, x_2, \ldots, x_n) \times \frac{1}{n} \times \sum_{i=1}^{n} x_i\right]^{\frac{1}{2}} \tag{10}$$

$$D(x) = 1 - C(1 - x) \tag{11}$$

The conjunction and disjunction defined by Eqs. 10 and 11 satisfy the CFL properties (a) to (g) [6], and they can be used to define new compensatory morphological operators [4]. In posterior chapters, we will prove how these new operators comply with the some of the properties required for a mathematical morphology, as defined in [2].

3.3 Software implementation

As a result of this work, we developed a software library, with efficient implementation of the operators, providing also a user-friendly image processing program. This development also filled the lack of existence of image processing software focused on the FMM and CFMM. This tool should help greatly to the design of prototypes for image processing tasks based on FMM. This development was done with Matlab© as programming language, resulting on a library and a graphical interface for image processing, with a wide range of MM, FMM and CFMM operators [8]. This tool provides extensive visualization capabilities, allowing the interactive design of algorithms. More classical image processing techniques were also included, to complement the morphological operators in the design of full image processing solutions.

3.4 Applications

Previous results include the detection of vascular trees in retinal images using CFMM [7] and the tracking of bacteria movements in dynamic speckle laser images using CFMM [23]. In [9], we propose a new linguistic representation of CFMM dilation and erosion operators, in a way that they can be associated with colloquial language. The proposal consists on replacing the supremum and infimum by the “existential” quantifier and the "for all" quantifier, respectively. Additionally, we applied CFMM to quantify the cover area of a surface coated by spray, measuring the profile deposition area from the completely cover surface, to the edge of the spray cone [24], and applied CFMM operators to the segmentation of lateral ventricles in MRI [10].

4 Compensatory fuzzy mathematical morphology based on arithmetic mean

In a previous section, we presented the equations for compensatory dilation and erosion, for an image μ with a SE ν, which were defined by Eqs. 8 and 9, where C and D are the compensatory conjunction and disjunction, respectively. Replacing these operators by the conjunction and disjunction of the AMBCFL, given by Eqs. 10 and 11, we can define new morphological operators:

$$\delta(\mu,\nu)(x) = \sup_{y\in U_\nu} \left[\min(\mu(y),\nu(y-x))\ldots \ldots \frac{\mu(y)+\nu(y-x)}{2}\right]^{\frac{1}{2}} \quad (12)$$

$$\varepsilon(\mu,\nu)(x) = \inf_{y\in U_\nu} \left\{1-\left[\min(1-\mu(y),\nu(y-x))\ldots \ldots \frac{1-\mu(y)+\nu(y-x)}{2}\right]^{\frac{1}{2}}\right\} \quad (13)$$

The duality between (12) and (13) results from the known duality between C and D. We must prove that these operators verify the four principles proposed by Serra in [25] (that Bloch and Maître translated to fuzzy language [2]). In the following section, we show that the new operators, defined in Eqs. 12 and 13, generate a FMM. Because the operations of conjunction and disjunction are operations of CFL, we call the morphology based on these operators as *Compensatory Fuzzy Mathematical Morphology*.

4.1 First principle: translation invariance

The first principle establishes that a transformation of fuzzy sets φ is translation invariant if $\forall\mu\in M, \forall t\in S, \varphi(\mu+t) = [\varphi(\mu)]+t$, where $\mu+t$ is a fuzzy set whose membership function μ is translated by t, that is to say: $\forall x\in S$ $(\mu+t)(x) = \mu(x+t)$. It is important to clarify that M is the space of all fuzzy sets and S is the domain of the membership function $\mu : S\to[0,1]$. Since the same SE is used everywhere in space, the translation invariance is directly derived. Therefore:

$$\delta(\mu,\nu)+t = \delta(\mu+t,\nu) \quad (14)$$

$$\varepsilon(\mu,\nu)+t = \varepsilon(\mu+t,\nu) \quad (15)$$

4.2 Second principle: compatible with homothesis

A transformation of fuzzy sets φ is compatible with homothesis if $\varphi(\lambda\mu) = \lambda\varphi(\mu)$, $\forall\mu\in M$, $\forall\lambda\in(0,1]$, where $(\lambda\mu)(x) = \lambda\mu(x)$. This principle is not satisfied for the new operators of the CFMM, as shown by the following example: let be $\lambda = 0.5$, $a = 0.3$ and $b = 0.6$:

$$C(\lambda a,b) = 0.2372 \quad \lambda C(a,b) = 0.1837$$

$$D(\lambda a,b) = 0.2929 \quad \lambda D(a,b) = 0.2655$$

Thus, $C(\lambda a,b) \neq \lambda C(a,b)$ and $D(\lambda a,b) \neq \lambda D(a,b)$. However, property 2 does not need to be strongly imposed, because for fuzzy sets, compatibility with homothesis can be avoided [2,11].

4.3 Third principle: local knowledge

The fuzzy equivalent to the third principle of MM can be expressed as follows: Let μ and ν be two fuzzy subsets of S and let σ be a set a bounded set of S such that $\mu\bigcap\sigma$ is known. Then, the fuzzy erosion and dilation verified the local knowledge if a bounded set σ' of S exists and it depends only of σ such that $\varepsilon(\mu\bigcap\sigma,\nu)\bigcap\sigma' = \varepsilon(\mu,\nu)\bigcap\sigma'$ and $\delta(\mu\bigcap\sigma,\nu)\bigcap\sigma' = \delta(\mu,\nu)\bigcap\sigma'$.

To show that the third principle is satisfied, we will use the following theorem [11]:

Theorem 1 *Let μ and ν fuzzy subsets of S, let σ be any bounded classic set of S in which $\mu\bigcap\sigma$ is known and let I be a fuzzy implication decreasing with respect to the first variable and increasing in the second variable and verifying $I(0,b) = 1$ $\forall b\in[0,1]$. Then, the following two equalities are satisfied:*

1. $\varepsilon(\mu\bigcap\sigma,\nu)\bigcap\varepsilon(\sigma,\nu_{\circ\alpha}) = \varepsilon(\mu,\nu)\bigcap\varepsilon(\sigma,\nu_{\circ\alpha})$
2. $\delta((\mu\bigcap\sigma)\bigcup\sigma^C,\nu)\bigcap\varepsilon(\sigma,(-\nu)_{\circ\alpha}) = \ldots$

$$\ldots = \delta(\mu\bigcap\sigma,\nu)\bigcap\varepsilon(\sigma,(-\nu)_{\circ\alpha})$$

being $\nu_{\circ\alpha} = \bigcup_{\alpha\in]0,1]}\nu_\alpha$.

To show that the compensatory erosion of the CFMM verifies this principle, we use the fact that it is defined from implication (Eq. 2) as:

$$\varepsilon(\mu,\nu)(x) = \inf_{y\in U_\nu}[I(\nu(y-x),\mu(y))]$$

Therefore, it must be shown that the implication used in the definition of erosion is decreasing in the first argument, increasing in the second argument and that it verifies $I(0,b) = 1\forall b\in[0,1]$.

In first place, we show that it is decreasing in the first argument: let be $a\leq a^*$, then:

$$\min(a, 1-b) \leq \min(a^*, 1-b) \wedge \frac{(a+1-b)}{2} \leq \frac{a^*+1-b}{2}$$
$$\left[\min(a, 1-b)\frac{(a+1-b)}{2}\right]^{\frac{1}{2}} \leq \left[\min(a^*, 1-b)\frac{(a^*+1-b)}{2}\right]^{\frac{1}{2}}$$
$$1-\left[\min(a, 1-b)\frac{(a+1-b)}{2}\right]^{\frac{1}{2}} \geq 1-\left[\min(a^*, 1-b)\frac{(a^*+1-b)}{2}\right]^{\frac{1}{2}}$$
$$D(N(a), b) \geq D(N(a^*), b) \Rightarrow I(a, b) \geq I(a^*, b)$$

In second place, we prove that it is decreasing in the second argument: let be $b \leq b^*$, then:

$$\min(a, 1-b) \geq \min(a, 1-b^*) \wedge \frac{(a+1-b)}{2} \geq \frac{a+1-b^*}{2}$$
$$\left[\min(a, 1-b)\frac{(a+1-b)}{2}\right]^{\frac{1}{2}} \geq \left[\min(a, 1-b^*)\frac{(a+1-b^*)}{2}\right]^{\frac{1}{2}}$$
$$1-\left[\min(a, 1-b)\frac{(a+1-b)}{2}\right]^{\frac{1}{2}} \leq 1-\left[\min(a, 1-b^*)\frac{(a+1-b^*)}{2}\right]^{\frac{1}{2}}$$
$$D(N(a), b) \leq D(N(a), b^*) \Rightarrow I(a, b) \leq I(a, b^*)$$

Finally, we show that it satisfies the condition requested:

$$I(0, b) = D(N(0), b) = D(1, b) = \ldots$$
$$\ldots = 1-\left[\min(0, 1-b)\frac{1-b}{2}\right]^{\frac{1}{2}} = 1$$

Thus, the erosion of the CFMM satisfies the conditions of the theorem; therefore, it satisfies the principle of local knowledge. The proof for dilation is similar.

4.4 Fourth principle: morphological transformations semicontinuity

The following theorem, whose proof can be found in [11], suggests that if the fuzzy implication used in the definition of the operators is semicontinuous, then the operator is semicontinuous.

Theorem 2 *Let I be a fuzzy implication* $I : [0, 1] \times [0, 1] \rightarrow [0, 1]$ *that is decreasing in the first argument, increasing in the second argument and semicontinuous. Then, the fuzzy erosion is semicontinuous, that is* $\forall x \in U$*:*

$$\varepsilon\left(\sup_{i\in N}\mu^i, \inf_{j\in N}\nu^j\right)(x) = \inf_{i,j\in N}\varepsilon(\mu^i, \nu^j)(x)$$

To meet the conditions of this theorem, the fuzzy implication needs to be semicontinuous, because it was already shown that it is decreasing in the first argument and increasing in the second. To show semicontinuity, it is easy to verify:

$$\overline{\lim} I(a_i, b_j) = \inf_{n\geq 0}\sup_{i,j\geq n} I(a_i, b_j) = I\left(\sup_{i\in N}(a_i), \inf_{j\in N}(b_j)\right)$$

Therefore, $\overline{\lim} I(a_i, b_j)$ is bounded, and the implication is semicontinuous. As a result, the compensatory erosion is a semicontinuous operator. From duality between operators, it follows that the compensatory dilation is also semicontinuous.

Therefore, for erosion and dilation of the CFMM, three of the four principles of mathematical morphological, extended to FMM in [2], hold true.

5 Robustness analysis

If an operator is heuristically defined to handle a task, robustness is a desirable feature, since it means that the end result would not be affected by noise on the images. For this analysis, we used MRI, because they are one of the fields of interest in biomedical imaging, and noise is one common issue in this type of images. Therefore, in this section we analyze the robustness of the basic operators against noise in the images, comparing classic MM, FMM and CFMM. The evaluation is based on measuring how much the result, over noisy images, is different from the result when the operators are applied on the original, noiseless, images.

5.1 Materials and methods

We call I the original noiseless image, and I_λ the noisy image, obtained by applying a noise model on I. Let λ a parameter that controls the amount of noise in the model, for example the standard deviation for white noise, where $\lambda = \sigma^2$. To measure the amount of change in the resulting image, after application of the operator ψ, we define $\mathcal{E}_\lambda$ as the *difference* between $\psi(I)$ and $\psi(I_\lambda)$. The difference is measured by the mean square error between the two images: $\mathcal{E}_\lambda = MSE(\psi(I), \psi(I_\lambda))$. A low value of $\mathcal{E}_\lambda$ indicates a high similarity between these images, indicating that the noise did not affect noticeably the operator.

Since the noise was randomly generated, we averaged the results over the 100 repeats. Finally, the same analysis was repeated over 10 different MRI. Additionally, in the definition of FMM some norms are based on a parameter γ, which was selected based on the previous experience.

The operators used in the analysis consisted in dilation and erosion, since most of the morphological operators are based on these two. Because they are completely defined by their SE, we used different SE sizes. The technical details are described in the following list:

- Images: the ten images used were MRI acquired with a Tesla 1.5 equipment. The protocol included coronal and axial images, weighted in T2 (TR = 3500 ms, TE! = 32 ms, TE = 96 ms).

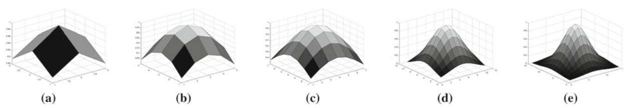

Fig. 1 Fuzzy structuring elements used in the analysis. **a** 3×3. **b** 5×5. **c** 7×7. **d** 11×11. **e** 15×15

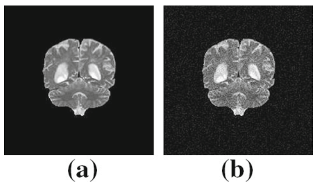

Fig. 2 **a** Original image. **b** Noisy image ($\sigma^2 = 300$)

- FMM: the six different norms used to define the fuzzy operators are algebraic (T1-S1), standard (T2-S2), bounded (T3-S3), drastic (T4-S4), Dubois & Prade (T5-S5) and Hamacher (T6-S6) [5].
- CFMM: the two definitions of compensatory morphology used are defined by Eqs. 4, 5, 10 and 11. C1 and D1 denote the operators of the GMBCFL. C2 and D2 denote the operators of the AMBCFL.
- Noise: the noise used follows an additive Gaussian model $N(0, \sigma^2)$, with six different variance values: $\sigma^2 = \{50, 100, 150, 200, 250, 300\}$.
- Repeats: the analysis was repeated 100 times, generating new instances of the random noise each time.
- Operators: dilation and erosion.
- Structuring Element: we used five different symmetric fuzzy structuring elements, of size 3×3, 5×5, 7×7, 11×11 and 15×15. The shape of these elements was defined by a Gaussian function centered on the SE center, as shown in Fig. 1. In the case of MM, the flat SE was defined as an square of the same size of each fuzzy SE.
- FMM parameter: for these FMM models that need a parameter γ (Dubois & Prade and Hamacher), the value used was $\gamma = 0.2$.

5.2 Results

In this section, we present the results of the robustness analysis performed. As an example of results, Fig. 2 shows an original image and the associated noisy image (for a value of $\sigma^2 = 300$), and Fig. 3 shows the results of the dilation operator of these two images, for MM, CFMM and FMM (using the Bounded norm), using a 7×7 structuring element. Figure 4 shows the results of the erosion operator, for the same models.

Figures 5 and 6 show, as an example, the plot of mean square error (MSE) against noise level for SE of dimension 3×3 and 15×15. In each graph, the different models are displayed in different colors. The vertical interval on each

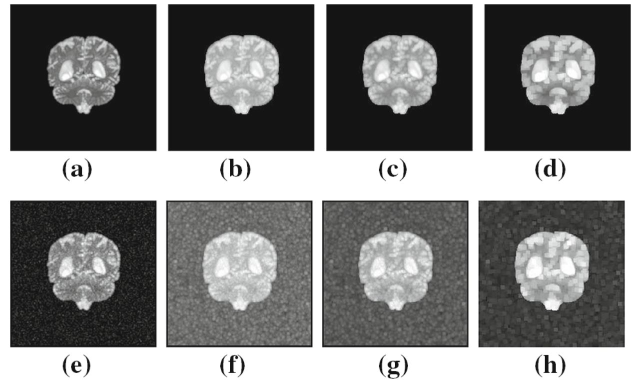

Fig. 3 Dilation of the original and noisy images: **a–e** FMM using the Bounded norm, **b–f** CFMM based on geometric mean, **c–g** CFMM based on arithmetic mean, **d–e** MM

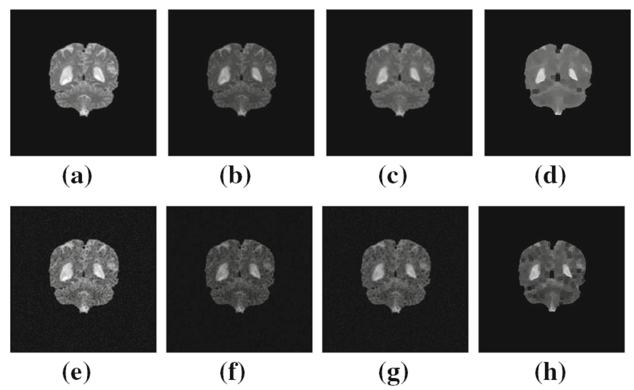

Fig. 4 Erosion of the original and noisy images: **a–e** FMM using the Bounded norm, **b–f** CFMM based on geometric mean, **c–g** CFMM based on arithmetic mean, **d–e** MM

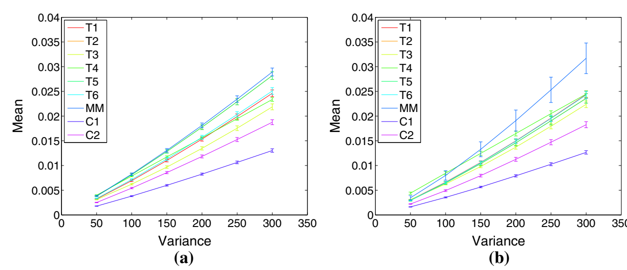

Fig. 5 MSE for dilation for different SE size. **a** 3×3. **b** 15×15

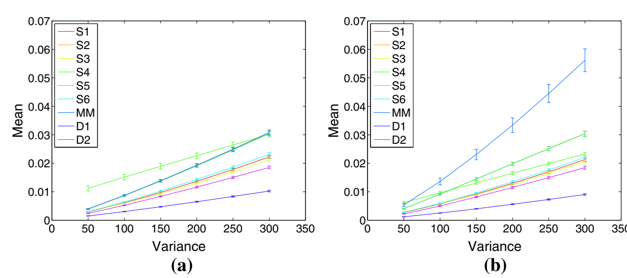

Fig. 6 MSE for erosion for different SE size. **a** 3×3. **b** 15×15

Table 1 Lowest error for dilation

SE	$\sigma^2 = 50$	$\sigma^2 = 150$	$\sigma^2 = 300$
3×3	$(C1)$ 0.0017772	$(C1)$ 0.0059891	$(C1)$ 0.013032
5×5	$(C1)$ 0.0016542	$(C1)$ 0.0057433	$(C1)$ 0.012841
7×7	$(C1)$ 0.0016301	$(C1)$ 0.0056658	$(C1)$ 0.012691
11×11	$(C1)$ 0.0016262	$(C1)$ 0.0056506	$(C1)$ 0.012685
15×15	$(C1)$ 0.0016227	$(C1)$ 0.0056469	$(C1)$ 0.012656

The name of the operators that reached the minimum is denoted between parentheses next to the error

Table 2 Highest error for dilation

SE	$\sigma^2 = 50$	$\sigma^2 = 150$	$\sigma^2 = 300$
3×3	$(T4)$ 0.0039898	(MM) 0.01306	(MM) 0.02892
5×5	$(T4)$ 0.0044384	(MM) 0.01437	(MM) 0.03323
7×7	$(T4)$ 0.0044487	(MM) 0.01440	(MM) 0.03387
11×11	$(T4)$ 0.0044098	(MM) 0.01363	(MM) 0.03285
15×15	$(T4)$ 0.0043956	(MM) 0.01327	(MM) 0.0317

The name of the operators that reached the maximum is denoted between parentheses next to the error

Table 3 Lowest error for erosion

SE	$\sigma^2 = 50$	$\sigma^2 = 150$	$\sigma^2 = 300$
3×3	$(D1)$ 0.001479	$(D1)$ 0.004716	$(D1)$ 0.010246
5×5	$(D1)$ 0.001244	$(D1)$ 0.004175	$(D1)$ 0.009376
7×7	$(D1)$ 0.001194	$(D1)$ 0.004024	$(D1)$ 0.009090
11×11	$(D1)$ 0.001187	$(D1)$ 0.003998	$(D1)$ 0.009043
15×15	$(D1)$ 0.001187	$(D1)$ 0.003999	$(D1)$ 0.009028

The name of the operators that reached the minimum is denoted between parentheses next to the error

Table 4 Highest error for erosion

SE	$\sigma^2 = 50$	$\sigma^2 = 150$	$\sigma^2 = 300$
3×3	$(S4)$ 0.011203	$(S4)$ 0.018936	(MM) 0.03083
5×5	$(S4)$ 0.008249	$(S4)$ 0.015487	(MM) 0.04155
7×7	$(S4)$ 0.0063565	(MM) 0.02060	(MM) 0.04847
11×11	$(S4)$ 0.0061401	(MM) 0.02285	(MM) 0.05514
15×15	$(S4)$ 0.0061705	(MM) 0.02306	(MM) 0.05619

The name of the operators that reached the maximum is denoted between parentheses next to the error

value represents the standard deviation of the computed MSE values, over the 100 iterations.

Table 1 shows for each value of σ^2 and SE, the MSE for the best operator (lowest MSE), which is indicated between parentheses next to the error values, when using the dilation operator. In the same way, Table 2 shows the MSE for the worst operator. Tables 3 and 4 describe the same results for the erosion operator.

Finally, Figs. 7 and 8 show the boxplots of the computed MSE values. For each noise level, there is a boxplot describing the average and deviation of the MSE values. They describe graphically the errors for MM, FMM (based on the Bounded norm) and the CFMM based on geometric mean.

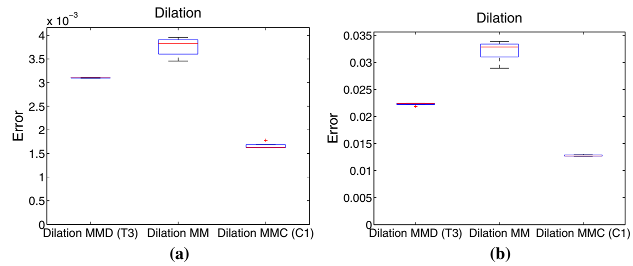

Fig. 7 *Boxplots* for dilation for several values of variance. **a** $\sigma^2 = 50$. **b** $\sigma^2 = 300$

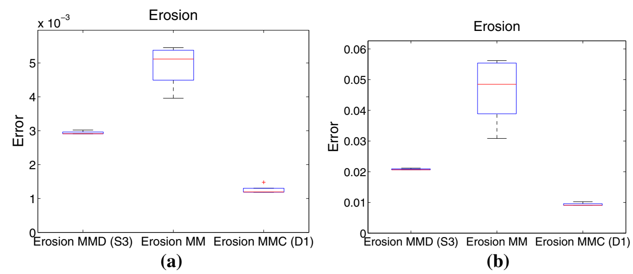

Fig. 8 *Boxplots* for erosion for several values of variance. **a** $\sigma^2 = 50$. **b** $\sigma^2 = 300$

5.3 Discussion

Regarding performance, Tables 1 and 3 show that CFMM based on geometric mean has the best performance against noise. Figures 5 and 6 show also that the CFMM based on arithmetic mean performance is better than MM and all the tested FMM.

On the other hand, Tables 2 and 4 show that MM performs worse than Fuzzy operators, except for small amount of noise, where the Drastic FMM has worse performance (differently from other FMM norms, the Drastic FMM is based on a non-continuous function).

Regarding FMM, the Bounded norm shows the best overall performance, while Dubois & Prade and Standard show very similar results, which can be understood because their t-norms and s-norms are very similar.

With respect to the SE size, for erosions, the larger is the SE size, the stronger results the sensibility to noise. This behavior is not observed for dilation. This shows that robustness against noise is dependent on the SE size for erosions, but not for dilation.

6 Conclusions

The MM has been broadly used to solve segmentation challenges in biomedical images, where noise and uncertainty are important factors, influencing directly on the performance of the algorithms. In this work, we presented new operators of the CFMM using CFL based on arithmetic mean, which satisfy three of the four principles of the MM and handle these factors by using Compensatory Logic, adding potentially the ability to obtain better results in this kind of images.

The simulation analysis showed that the CFMM operators display, for the model used here, better robustness against noise than FMM and MM operators. It is be expected that more complex operators, based on CMM, are also more robust against noise than the ones constructed from MM or FMM.

Finally, a library of CFMM operators, and a graphical user interface, were developed for further usage in analysis and applications. The GUI includes also Digital Image Processing general techniques for a more complete image processing.

As a future work, we will analyze for which type of situations, like different noise models, the operators are better adapted. Additionally, some important properties of mathematical morphology operators, in particular adjunctions, are of great importance for the development of a formal theory and should be treated in the future. Moreover, considering the importance of quantifiers for CFL, we expect to be able to advance in the definition of new morphological operators based on hybrid models.

References

1. Aptoula, E., Lefévre, S.: α-trimmed lexicographical extrema for pseudo-morphological image analysis. J. Visual Commun. Image Represent. **19**(3), 165–174 (2008)
2. Bloch, I., Maître, H.: Fuzzy mathematical morphologies: a comparative study. Pattern Recognit. **28**, 1341–1387 (1995)
3. Bloch, I.: Fuzzy sets for image processing and understanding. Fuzzy Sets Syst. **281**(C), 280–291 (2015)
4. Bouchet, A., Pastore, J., Brun, M., Ballarin, V.: Lógica Difusa Compensatoria basada en la media aritmética y su aplicación en la Morfología Matemática Difusa, 4to Torneo Regional de Inteligencia Computacional, IEEE (2010)
5. Bouchet, A., Pastore, J., Andrade, R.E., Brun, M., Ballarin, V.: Compensatory logic applied to digital image processing. In: Andrade, R.E., Gómez, J., Valdéz, A. (eds.) Towards a Trans-Disciplinary Technology of Business and Organizational Intelligence: Gathering Knowledge Discovery, Knowledge Management and Decision, pp. 226–239. Shaker Verlag, Aachen, University of Oldenburg, Alemania (2011)
6. Bouchet, A., Pastore, J.I., Espín Andrade, R., Brun, M., Ballarin, V.: Arithmetic mean based compensatory fuzzy logic. Int. J. Comput. Intell. Appl. **10**, 231–243 (2011)
7. Bouchet, A., Pastore, J., Espín Andrade, R., Brun, M., Ballarin, V.: Morfología Matemática Compensatoria aplicada a la segmentación de imágenes médicas, Tercer Taller Internacional de Descubrimiento de Conocimiento, Gestin del Conocimiento y Toma de Decisiones, Universidad de Cantabria y Universidad de Oldenburgo, España (2011)
8. Bouchet, A., Comas, D., Pastore, J., Brun, M., Ballarin, V.: Fuzzy mathematical morphology toolbox and graphical interface. IEEE Latin Am. Trans. **11**, 1090–1096 (2013)
9. Bouchet, A., Meschino, G., Brun, M., Espín Andrade, R., Ballarin, V.: Linguistic interpretation of mathematical morphology. In: Leyva López, J.C., Espin Andrade, R.A., Bello Pérez, R., Álvarez Carrillo, P.A. (eds.) Advances in Intelligent Systems Research, vol. 51, pp. 8–16. Atlantis Press, New York (2013)
10. Bouchet, A., Pastore, J., Brun, M., Ballarin, V.: Segmentation of lateral ventricles in magnetic resonance images. In: Braidot, A., Hadad, A. (eds.) IFMBE Proceedings, vol. 49, pp. 457–460. Springer, Berlin (2015)
11. Burillo López, P., Frago, N.P., Fuentes-Gonzlez, R.: Generation of fuzzy mathematical morphologies. Mathw. Soft Comput. **8**, 31–46 (2001)
12. Coliban, R., Ivanovici, M., Szekely, I.: Fast probabilistic pseudo-morphology for noise reduction in color images. Proced. Technol. **22**, 870–877 (2016)
13. De Baets, B., Kerre, E., Gupta, M.: The fundamentals of fuzzy mathematical morphology. Part 1: basic concepts. Int. J. Gen. Syst. **23**, 155–171 (1995)
14. De Baets, B., Kerre, E., Gupta, M.: The fundamentals of fuzzy mathematical morphology. Part 2: idempotence, convexity and decomposition. Int. J. Gen. Syst. **23**, 307–322 (1995)
15. Di Gesu, V., Maccarone, M.C., Tripiciano, M.: Mathematical morphology based on fuzzy operators. In: Lowen, R., Roubens, M. (eds.) Fuzzy Logic, pp. 477–486. Kluwer Academic Publishers, Berlin (1993)
16. Dubois, D., Prade, H.: Fuzzy Sets and Systems: Theory and Applications. Academic Press Inc, New York (1980)
17. Espín Andrade, R., Fernández González, E.: La Lógica Difusa Compensatoria: Una Plataforma para el Razonamiento y la Representacin del Conocimiento en un Ambiente de Decisión Multicriterio, Análisis Multicriterio para la Toma de Decisiones: Métodos y Aplicaciones. Coedición: editorial Plaza y Valdes / Editorial Universidad de Occidente (2009)
18. Espín Andrade, R., González Caballero, E., Pedrycz, W., Fernández González, E.R.: Archimedean-compensatory fuzzy logic systems. Int. J. Comput. Intell. Syst. **8**(2), 54–62 (2015)
19. Kerre, E.E., Nachtegael, M.: Fuzzy Techniques in Image Processing. Physica, New York (2000)
20. Klement, E.P., Mesiar, R., Pap, E.: Triangular norms. Position paper I: basic analytical and algebraic properties. Fuzzy Sets Syst. **143**, 5–26 (2004)
21. Menger, K.: Statistical metrics. Proc. Natl Acad. Sci. (PNAS) **28**(12), 535–537 (1942)
22. Nachtegael, M., Kerre, E.E.: Connections between binary, gray-scale and fuzzy mathematical morphologies. Fuzzy Sets Syst. **124**(1), 73–85 (2001)
23. Nisenbaum, M., Bouchet, A., Guzmán, M., González, J.F., Sendra, G.H., Pastore, J., Trivi, M., Murialdo, S.E.: Dynamic laser speckle and fuzzy mathematical morphology applied to studies of chemotaxis towards hydrocarbons. Int. J. Environ. Health **7**, 58–69 (2014)
24. Omar, S.A., Bouchet, A., Pellice, S., Ballarin, V., Ceré, S.M., Ballarre, J., Pastore, J.: Optimization of new spray technique for hybrid sol-gel coatings: preliminary deposition study. In: UNER (Ed.) VI Latin American Conference in Biomedical Engineering, Paraná, Entre Ríos, pp. 653–656 (2014)
25. Serra, J.: Image Analysis and Mathematical Morphology, vol. 1. Academic Press, London (1982)
26. Serra, J.: Image Analysis and Mathematical Morphology, vol. 2. Academic Press, London (1988)
27. Zadeh, L.A.: From computing with numbers to computing with words from manipulation of measurements to manipulation of perceptions. IEEE Trans. Circuits Syst. **45**, 105–119 (1999)